

31. C. A. Brochu, *J. Vertebr. Paleontol. Mem.* **22**, 1 (2003).
 32. We thank M. Norell and C. Mehling of the American Museum of Natural History and J. Gardner of the Royal Tyrrell Museum of Palaeontology for access to specimens in their care, and P. Larson and the Black Hills Institute of Geological Research Inc. for providing graphics for our

use. Supported by NSF Division of Earth Sciences grant EAR 0207744 (G.M.E.).

Supporting Online Material

www.sciencemag.org/cgi/content/full/313/5784/213/DC1
 Materials and Methods

Figs. S1 to S4
 Tables S1 to S4
 References

2 February 2006; accepted 1 June 2006
 10.1126/science.1125721

Crystal Structure of Glycoprotein B from Herpes Simplex Virus 1

Ekaterina E. Heldwein,^{1,2*} Huan Lou,⁴ Florent C. Bender,⁴ Gary H. Cohen,⁴
 Roselyn J. Eisenberg,⁵ Stephen C. Harrison^{1,2,3}

Glycoprotein B (gB) is the most conserved component of the complex cell-entry machinery of herpesviruses. A crystal structure of the gB ectodomain from herpes simplex virus type 1 reveals a multidomain trimer with unexpected homology to glycoprotein G from vesicular stomatitis virus (VSV G). An α -helical coiled-coil core relates gB to class I viral membrane fusion glycoproteins; two extended β hairpins with hydrophobic tips, homologous to fusion peptides in VSV G, relate gB to class II fusion proteins. Members of both classes accomplish fusion through a large-scale conformational change, triggered by a signal from a receptor-binding component. The domain connectivity within a gB monomer would permit such a rearrangement, including long-range translocations linked to viral and cellular membranes.

Herpes simplex virus type 1 (HSV-1) is the prototype of the diverse herpesvirus family, which includes such notable human pathogens as cytomegalovirus (CMV), Epstein-Barr virus (EBV), and Kaposi's sarcoma-associated herpesvirus (KSHV). Herpesviruses have an envelope, an outer lipid bilayer, bearing 12 surface glycoproteins. To deliver the capsid containing the double-stranded DNA genome into the host cell, HSV-1 must fuse its envelope with a cellular membrane. Among viral glycoproteins, only gC, gB, gD, gH, and gL participate in viral cell entry, and only the last four are required for fusion (1–4). All herpesviruses have gB, gH, and gL, which constitute the core fusion machinery (5). Of these, gB is the most highly conserved.

The virus attaches to a cell through a non-essential interaction of gC with heparan sulfate proteoglycan and through an essential interaction of gD with one of three cellular receptors: nectin-1, herpesvirus entry mediator (HVEM), or a specifically modified heparan sulfate (6). Crystal structures of the soluble ectodomain of gD, unbound and in complex with the ectodomain of HVEM (7, 8), show that binding of gD and receptor causes the former to undergo a conformational change in which a C-terminal segment of the ectodomain polypeptide chain is released from a strong intramolecular contact.

The liberated C-terminal segment may interact with gB or the gH/gL complex to trigger molecular rearrangements and, ultimately, fusion. The

precise functions of gB and gH/gL are unknown. Both are required for entry, and either or both presumably receive the signal from gD and respond by undergoing a conformational change; gD itself is thought not to participate in the fusion process (9, 10). Neither gB nor gH/gL has an obvious fusion peptide, but an indication that gB might be a fusion effector comes from the notable syncytial phenotype caused by certain mutations within the cytoplasmic domain of gB (1, 11–13).

HSV-1 gB is a 904-residue protein. In the work reported here, we determined the crystal structure of a nearly full-length ectodomain of gB, residues Asp¹⁰³ to Ala⁷³⁰ (14) (Fig. 1). Various features of the structure suggest that it is a fusion effector, an inference strengthened by its notable and unanticipated similarity to the structure of the fusion glycoprotein Gr of vesicular stomatitis virus (VSV), described in an accompanying paper (15). Domains that

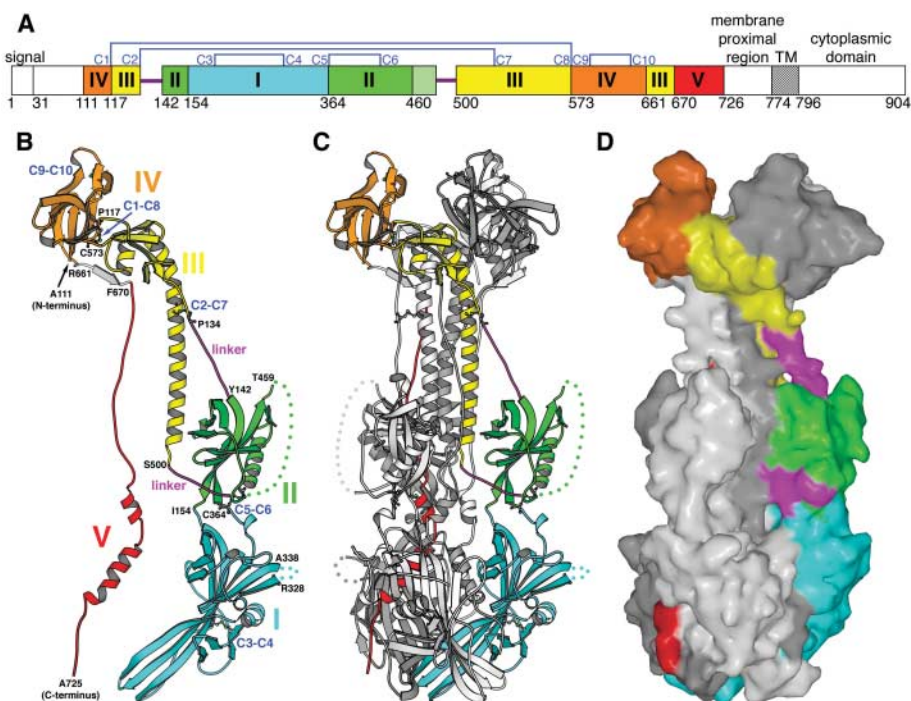


Fig. 1. (A) Domain architecture of gB. Domains observed in the crystal structure are highlighted in different colors, and their corresponding first residue positions are shown. (B) Ribbon diagram of a single gB protomer. The domains are rendered in colors corresponding to (A). Labeled residues (26) indicate the limits of individual domains and the disordered loop in domain I. Residues Arg⁶⁶¹ to Thr⁶⁶⁹ of the shown protomer are in gray because they belong to domain III of a neighboring protomer. Residues Arg⁶⁶¹ to Thr⁶⁶⁹ of the other neighboring protomer are included here and shown in yellow, because they contribute to a sheet in domain III of the shown protomer. Disordered segments are shown as dots of appropriate color. Disulfides are shown in ball-and-stick representation. Cysteines are numbered according to (A) and fig. S2. (C) gB trimer. Protomer A is the same as in (B). Protomer B is shown in white and protomer C in gray. (D) Accessible surface area representation of gB trimer. The coloring scheme is the same as in the rest of Fig. 1. Images were generated with the use of MOLSCRIPT (27) and SPOCK (28).

¹Department of Biological Chemistry and Molecular Pharmacology, Harvard Medical School, ²Laboratory of Molecular Medicine, ³Howard Hughes Medical Institute, Children's Hospital, 320 Longwood Avenue, Boston, MA 02115, USA. ⁴Department of Microbiology, School of Dental Medicine, ⁵Department of Pathobiology, School of Veterinary Medicine, University of Pennsylvania, 240 South 40th Street, Philadelphia, PA 19104, USA.

*To whom correspondence should be addressed. E-mail: heldwein@crystal.harvard.edu

cover the lateral surfaces of the gB spike are suspended by extended segments of polypeptide chain from the membrane-distal end of the molecule (Fig. 1), suggesting a mechanism for a fusogenic conformational change.

The crystal structure of the HSV-1 gB ectodomain, refined at 2.1 Å resolution, contains three protomers designated A, B, and C. Disordered regions correspond to ~10% of the polypeptide chain. Trimeric gB is a spike with approximate dimensions of 85 Å by 80 Å by 160 Å. The bulk of each protomer, residues Ala¹¹¹ to Thr⁶⁶⁹, coils around the others with a left-handed twist (Fig. 1). Each protomer extends a C-terminal arm from one end of the molecule to the other, inserting it into the junction between the other two protomers (Fig. 1). There is no trimerization domain per se; instead, multiple contacts between protomers throughout the molecule contribute to trimer stability. The 10 cysteines per subunit form five disulfide bonds, all intramolecular. Their pairwise assignments in our structure agree with those previously determined by mass spectrometry for a homologous HSV-2 gB (16).

Each protomer can be divided into five distinct regions or domains: I, base; II, middle; III, core; IV, crown; and V, arm (Fig. 1 and fig. S1). Residues Pro¹³⁴ to Asn¹⁴¹ and Val⁴⁹² to Ser⁴⁹⁹ are linkers between domains II and III.

Domain I is composed of a continuous polypeptide chain, residues Ile¹⁵⁴ to Val³⁶³ (Fig. 1). It has the fold characteristic of a pleckstrin-homology (PH) domain (17, 18), a β sandwich composed of two nearly orthogonal β sheets of four and three strands, respectively (Fig. 2). In cytoplasmic signaling pathways, proteins with this fold serve as scaffolds to allow phosphoinositide and peptide binding. The helix that in a canonical PH domain normally covers one opening of the β sandwich is replaced in domain I by a long loop and short helix. An insertion of residues Tyr¹⁶⁵ to Ile²⁷² between strands β 4 and β 11 creates a curving subdomain at the base of the trimer (Fig. 2). This latter subdomain consists of a four-strand β sheet (with three long strands and one short strand), the convex side of which is covered with an α helix, a β hairpin, and a short two-strand β sheet. This subdomain has no previously described structural relatives (19).

Domain II comprises two discontinuous segments, residues Tyr¹⁴² to Asn¹⁵³ and Cys³⁶⁴ to Thr⁴⁵⁹ (Fig. 1). At its center is a six-strand β barrel reminiscent of the PH superfold, with strand β 5 of the canonical PH domain missing (Fig. 2). In its place, there is a helix-strand insert on the outer face of the barrel. The entire domain I is inserted between strands β 3 and β 17, the first and second strands of domain II. Residues Leu⁴⁶⁰ to Ser⁴⁹¹ in protomers A and C and residues Glu⁴⁶² to Ser⁴⁹¹ in protomer B are disordered. Trypsin cleavage between Arg⁴⁷⁴ and Lys⁴⁷⁵ has probably destabilized this loop, which lies on the outer margin of domain II and which is the locus of a posttranslational cleav-

age in some herpesviruses, such as HCMV (20). The loop is at least partially ordered in crystals of uncleaved gB ectodomain (14).

Domain III contains three discontinuous segments, residues Pro¹¹⁷ to Pro¹³³, Ser⁵⁰⁰ to Thr⁵⁷², and Arg⁶⁶¹ to Thr⁶⁶⁹ (Fig. 1). It has a long, 44-residue α helix followed by a short helix and a small, four-strand mixed β sheet. The long helix and its trimeric counterparts form the central coiled-coil. Residues Arg⁶⁶¹ to Thr⁶⁶⁹ of the outer β strand do not belong to the same polypeptide chain but instead to a neighboring protomer. This region, which is not a domain in the strict sense of an independent folding unit, contributes many of the essential trimer contacts.

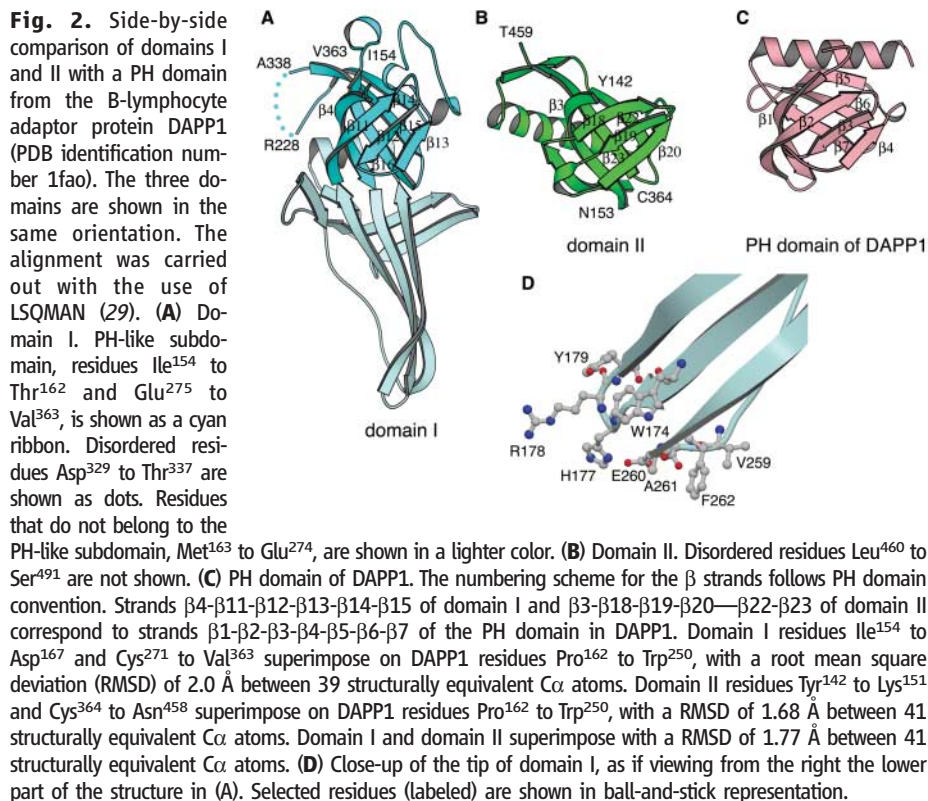
Domain IV comprises two discontinuous segments, residues Ala¹¹¹ to Cys¹¹⁶ and Cys⁵⁷³ to Ser⁶⁶⁰ (Fig. 1). These segments are linked by a disulfide bond, C1 to C8. This domain has no previously described structural relatives (19).

Domain V, residues Phe⁶⁷⁰ to Ala⁷²⁵, stretches from top to bottom of the molecule as a long extension (Fig. 1). Residues in this segment have no contact with the rest of the polypeptide chain of the same protomer but rather fit into the groove between the core domains of the other two protomers, probably reinforcing the trimer interactions.

gB is the most conserved herpesvirus entry glycoprotein (fig. S2). Our structure accounts well for the regions of high and low sequence variation. Thus, the structure of HSV-1 gB can be taken to represent the structure of all herpes-

virus gB proteins, and in analyzing properties such as antigenicity, we can map results from various herpesviruses onto it. Figure 3 shows several epitopes of neutralizing monoclonal antibodies against HSV and HCMV. All epitopes map to the surface, along the lateral faces of the spikes and on the tip of the crown. Although the majority of the epitopes are located far from either end of the molecule, two virus-neutralizing monoclonal antibodies to HSV, both of which recognize the same epitope, map to domain IV, directly on the crown end (21) (Fig. 3). In addition, residues Pro⁵⁷⁵ to Gln⁶⁵⁸ are homologous to antigenic domain 1 in HCMV gB, which is a dominant neutralizing epitope (22). Thus, we propose that on the surface of the virions, gB is oriented such that domain IV is fully exposed.

The gB ectodomain fragment we have analyzed lacked residues Ala³¹ to Arg¹⁰² and Met⁷³¹ to Asn⁷⁷³. Trypsin cleavage before crystallization separates residues Ala³¹ to Arg¹⁰², which are poorly conserved and relatively unstructured, from the rest of the molecule, probably because this segment, which contains a heparan sulfate interaction site (23), is not firmly anchored. We have determined a lower resolution (3.5 Å) structure of an uncleaved ectodomain trimer, residues Ala³¹ to Ala⁷³⁰ (14); the conformation of residues Thr¹⁰⁹ to Ala⁷²⁵ is essentially the same as in the crystals of trypsin-treated ectodomain, and the residues Ala³¹ to Asn¹⁰⁸ are disordered. The membrane-proximal region of the intact ectodomain, residues Met⁷³¹



to Asn⁷⁷³, is very hydrophobic. This characteristic suggests that it lies against the membrane, perhaps forming a pedestal for the rest of the trimeric ectodomain.

The complex architecture of the gB ectodomain identifies it as a homolog of VSV G, described in the accompanying paper (15). The VSV G ectodomain is smaller and more compact than gB, but the individual domains are structurally homologous (fig. S3) and their spatial relations correspond remarkably closely. The most obvious similarities include the elongated structural element that includes domains I and II of gB (corresponding to domains IV and III, respectively, in VSV G), the PH domain-like

fold of domain II (domain III in VSV G), the central helix of domain III of gB (domain II of VSV G), the order of strands of gB domain IV (domain I of VSV G), and the location of the C terminus adjacent to the putative fusion loops.

G, the sole surface protein on VSV, is the viral fusogen. It contains an internal fusion loop, identified by membrane photolabeling experiments (24) as the segment corresponding to the tip of our domain I. G undergoes a reversible, fusion-activating conformational change at low pH; the structural correlates of this change have not yet been mapped. The similarity to VSV G strongly suggests that gB is the effector of fusion in herpesviruses and

that aspects of the fusion mechanisms proposed for other viral fusion proteins apply. The two loops at the tip of domain I, corresponding to the fusion peptide segments in VSV G, contain hydrophobic residues, including an exposed phenylalanyl side chain and a tryptophanyl side chain that could rotate into an exposed position (Fig. 2). This tip could insert into the interface between head groups and hydrocarbons in a lipid bilayer, in the same way that the class II viral fusion loops insert (25). Nevertheless, the conformation of the fusion loops appears sub-optimal for membrane insertion, and we anticipate that local conformational changes will expose more hydrophobic residues.

An important characteristic of viral fusion effectors is triggered conformational rearrangement. In most cases, the transition is irreversible, and the structural change dramatic. Because the VSV G transition appears to be reversible and because the protein is a trimer in both states, the structural differences between the two states might be less striking. The structure of VSV G described in the accompanying paper is probably the postfusion form. Which state of gB does our structure represent? The epitopes for neutralizing antibodies all map to the surface of the protein in the conformation present in our crystals (Fig. 3). In particular, the major neutralizing epitope for HCMV gB lies on the outer face of the crown (domain IV). Neutralizing antibodies should recognize the prefusion conformation of gB, and we might expect that at least some of the epitopes would be absent from the surface of the protein in a postfusion conformation. Nonetheless, a number of other features suggest that our structure represents a postfusion state, consistent with its similarity to the low-pH form of VSV G. The critical characteristic of all postfusion structures, in both class I and class II fusion proteins, is adjacency of the fusion peptide and the C-terminal transmembrane anchor. The fusion peptide inserts into the target-cell membrane; the transmembrane anchor crosses the viral membrane, and the transition to proximity forces the two membranes together. The putative gB fusion loops are indeed adjacent to the C-termini of the polypeptide chains of the fragment we have crystallized, but there are about 45 additional residues not present in the expressed fragment that intervene between its terminus and the transmembrane segment. Uncertainty about the disposition of this intervening peptide thus makes it difficult to conclude where the transmembrane anchor will be relative to the tip of domain I. The peptide could be analogous to the stem of flavivirus fusion proteins: a hydrophobic element that forms a pedestal against the membrane in the prefusion state and zips up along the trimer in the transition to a postfusion state.

Some unusual features of the gB structure suggest that it has evolved to unfold and refold like other viral fusion proteins. Do-

Fig. 3. Accessible surface of the gB ectodomain in semi-transparent rendering in a side view (A) and a top view (B). The underlying polypeptide chains are shown as white worms. Three groups of epitopes of the neutralizing antibodies are shown. Group 1 contains epitopes in HSV-1 gB identified by isolating single-amino acid monoclonal antibody (mAb) resistance mutants. These are residues Ala³¹⁵ and Arg³²⁸ (mAb H233), shown in blue; residues Tyr³⁰³ (mAb H126), Arg³⁰⁴ (mAb H1375), Glu³⁰⁵ (mAb B4), and His³⁰⁸ (mAb H1435), shown in red; and residue Gly⁵⁹⁴ (mAbs B2 and B5), shown in green (21, 30–32). Group 2 contains epitopes in HSV-1 gB identified by peptide mapping using enzyme-linked immunosorbent assays (ELISAs). These are residues Ala³⁹⁰ to Gly⁴¹⁰ (mAb H1838), shown in cyan; residues Pro⁴⁵⁴ to Ser⁴⁷³ (mAb H1781), shown in yellow; and residues Ser⁶⁹⁷ to Ala⁷²⁵ (mAbs SS106 and SS144), shown in orange (14). Group 3 contains epitopes in HCMV gB identified by peptide mapping using ELISAs. These correspond to HSV-1 residues Pro⁵⁹³ to Val⁶⁰², Ala⁶²⁹ to Thr⁶⁴² (mAbs ITC48, ITC52, ITC63B, and ITC63C), and Glu⁶³¹ to Val⁶⁴⁸ (mAb 7-17), all shown in purple (33, 34). The orientations were chosen to show all the epitopes and were derived from the orientation in Fig. 1 by rotating the molecule about the vertical axis by $\sim 45^\circ$ to the left.

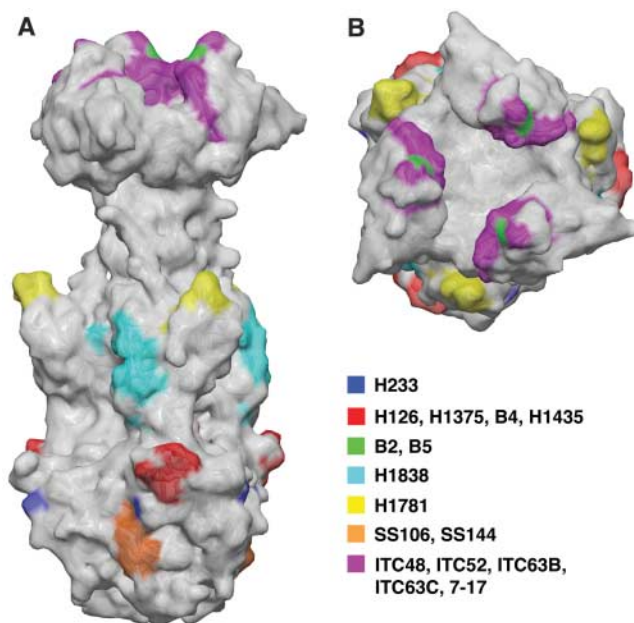
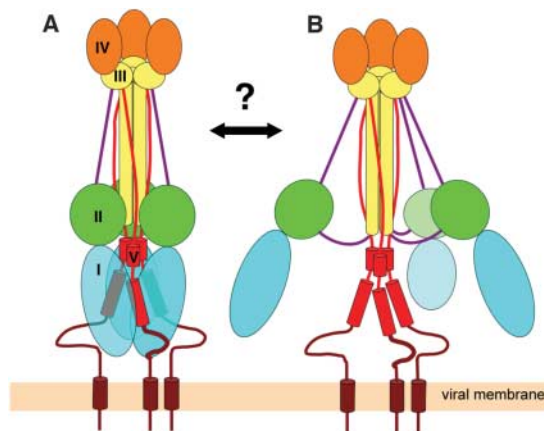


Fig. 4. Schematic model of gB, illustrating how it could refold in an umbrellalike fashion. (A) Structure determined in this work. Domains are shown schematically by using the color scheme in Fig. 1. The membrane-proximal regions are shown as brown lines. Transmembrane regions are shown as brown cylinders. (B) The linkers leading into and out of the domain I-II module would permit a large-amplitude rotation. The structure described here might represent either the starting point or the endpoint of such a translocation, and thus it might have either a prefusion or a postfusion conformation (double-headed arrow).



mains I and II, which decorate the lateral surface of the trimer, are suspended from the rest of the molecule by curiously extended polypeptide segments (Fig. 1 and Fig. 4). Moreover, they trap the almost fully extended domain V of another monomer. The segment that leads downward into domain II is anchored at the top by a disulfide bond to the coiled-coil, C2 to C7. The segment that leads out of domain II and into the coiled-coil contains the long disordered loop that is cleaved in CMV. These two linker segments would permit large motions of the domain I-II fusion module, as suggested in the diagram (Fig. 4). The putative fusion loops at the tip of this module could swing through a substantial arc.

Despite the notable homology between gB and VSV G, the two proteins have some functional differences. Unlike VSV G, gB alone is not sufficient for viral entry; all herpesviruses also require gH and gL. The trigger for HSV fusion is, at least in part, the rearrangement of gD induced by receptor binding. Receptor-mediated release of the gD C terminus would allow it to contact another HSV glycoprotein involved in entry, e.g., the peripherally located, PH-like domains I and II of gB. It is possible that gH/gL restrains gB in a prefusion state; the exposed gD C terminus might then interrupt this inhibitory contact at least in the case of alphaherpesviruses. Whatever the mechanism, the structure of gB identifies it as the fusogen and shows it to have the properties

needed for a fusion-promoting conformational rearrangement.

References and Notes

- W. H. Cai, B. Gu, S. Person, *J. Virol.* **62**, 2596 (1988).
- M. W. Ligas, D. C. Johnson, *J. Virol.* **62**, 1486 (1988).
- A. Forrester *et al.*, *J. Virol.* **66**, 341 (1992).
- C. Roop, L. Hutchinson, D. C. Johnson, *J. Virol.* **67**, 2285 (1993).
- P. G. Spear, R. Longnecker, *J. Virol.* **77**, 10179 (2003).
- P. G. Spear, *Cell. Microbiol.* **6**, 401 (2004).
- A. Carfi *et al.*, *Mol. Cell* **8**, 169 (2001).
- C. Krummenacher *et al.*, *EMBO J.* **24**, 4144 (2005).
- N. A. Jones, R. J. Geraghty, *Virology* **324**, 213 (2004).
- F. Cocchi *et al.*, *Proc. Natl. Acad. Sci. U.S.A.* **101**, 7445 (2004).
- P. J. Gage, M. Levine, J. C. Glorioso, *J. Virol.* **67**, 2191 (1993).
- T. P. Foster, J. M. Melancon, K. G. Kousoulas, *Virology* **287**, 18 (2001).
- D. J. Bzik, B. A. Fox, N. A. DeLuca, S. Person, *Virology* **137**, 185 (1984).
- Materials and methods are available as supporting material on Science Online.
- S. Roche, S. Bressanelli, F. A. Rey, Y. Gaudin, *Science* **313**, 187 (2006).
- N. Norais *et al.*, *J. Virol.* **70**, 7379 (1996).
- N. Blomberg, E. Baraldi, M. Nilges, M. Saraste, *Trends Biochem. Sci.* **24**, 441 (1999).
- M. A. Lemmon, K. M. Ferguson, *Biochem. J.* **350**, 1 (2000).
- L. Holm, C. Sander, *Trends Biochem. Sci.* **20**, 478 (1995).
- M. Vey *et al.*, *Virology* **206**, 746 (1995).
- S. L. Highlander *et al.*, *J. Virol.* **63**, 730 (1989).
- W. J. Britt, M. A. Jarvis, D. D. Drummond, M. Mach, *J. Virol.* **79**, 4066 (2005).
- S. Laquerre *et al.*, *J. Virol.* **72**, 6119 (1998).
- P. Durrer, Y. Gaudin, R. W. H. Ruigrok, R. Graf, J. Brunner, *J. Biol. Chem.* **270**, 17575 (1995).
- S. C. Harrison, *Adv. Virus Res.* **64**, 231 (2005).
- Single-letter abbreviations for the amino acid residues are as follows: A, Ala; C, Cys; D, Asp; E, Glu; F, Phe; G, Gly; H, His; I, Ile; K, Lys; L, Leu; M, Met; N, Asn; P, Pro; Q, Gln; R, Arg; S, Ser; T, Thr; V, Val; W, Trp; and Y, Tyr.
- P. J. Kraulis, *J. Appl. Crystallogr.* **24**, 946 (1991).
- More information is available online (<http://quorum.tamu.edu/Manual/Manual/Manual.html>).
- G. J. Kleywegt, T. A. Jones, *Acta Crystallogr.* **D52**, 826 (1996).
- P. E. Pellett, K. G. Kousoulas, L. Pereira, B. Roizman, *J. Virol.* **53**, 243 (1985).
- K. G. Kousoulas, B. Huo, L. Pereira, *Virology* **166**, 423 (1988).
- L. Pereira, M. Ali, K. Kousoulas, B. Huo, T. Banks, *Virology* **172**, 11 (1989).
- U. Utz, W. Britt, L. Vugler, M. Mach, *J. Virol.* **63**, 1995 (1989).
- M. Ohlin, V. A. Sundqvist, M. Mach, B. Wahren, C. A. Borrebaeck, *J. Virol.* **67**, 703 (1993).
- We thank M. Berne of the Tufts Protein Chemistry Facility for N-terminal sequencing, D. King of the University of California at Berkeley for mass spectrometry, E. Settembre for the x-ray data collection, E. M. Vogan for help with crystallographic software, and L. Pereira for providing several antibodies to gB. This work was funded by NIH grants AI065886 (to E.E.H.), AI049980 (to S.C.H.), and AI056045 and NS36731 (to R.J.E.). S.C.H. is an investigator in the Howard Hughes Medical Institute. Coordinates and structure factors have been deposited with the Research Collaboratory for Structural Bioinformatics (RCSB) Protein Data Bank (PDB) with accession code 2gum.

Supporting Online Material

www.sciencemag.org/cgi/content/full/313/5784/217/DC1

Materials and Methods

Figs. S1 to S3

Tables S1 and S2

References

22 February 2006; accepted 16 May 2006

10.1126/science.1126548

A Bacterial Virulence Protein Suppresses Host Innate Immunity to Cause Plant Disease

Kinya Nomura,¹ Sruti DebRoy,¹ Yong Hoon Lee,¹ Nathan Pumplin,¹ Jonathan Jones,² Sheng Yang He^{1*}

Plants have evolved a powerful immune system to defend against infection by most microbial organisms. However, successful pathogens, such as *Pseudomonas syringae*, have developed countermeasures and inject virulence proteins into the host plant cell to suppress immunity and cause devastating diseases. Despite intensive research efforts, the molecular targets of bacterial virulence proteins that are important for plant disease development have remained obscure. Here, we show that a conserved *P. syringae* virulence protein, HopM1, targets an immunity-associated protein, AtMIN7, in *Arabidopsis thaliana*. HopM1 mediates the destruction of AtMIN7 via the host proteasome. Our results illustrate a strategy by which a bacterial pathogen exploits the host proteasome to subvert host immunity and causes infection in plants.

Many plant and human pathogenic bacteria rely on an essential virulence system—the type III secretion system—to inject virulence effector proteins into the host cell to cause infection (1–3). Recent research has documented the ability of effector proteins of mammalian pathogenic bacteria

to modulate host cytoskeleton dynamics, membrane composition, vesicle trafficking, and host immunity (4). In contrast, very little is known about the molecular mechanisms by which bacterial effector proteins induce disease in plants. Emerging evidence suggests that a major function of these effector proteins

is to suppress host immune responses in susceptible plants (5–11). However, the mechanisms by which effector proteins subvert host immune responses are poorly understood at the molecular level.

Pseudomonas syringae infects a wide range of economically important plant species. All of the examined *P. syringae* strains contain a common genomic pathogenicity island, which is composed of type III secretion-associated *hrp/hrc* genes, an exchangeable effector locus, and a conserved effector locus (12). A partial deletion of the conserved effector locus in the Δ CEL mutant of *Pst* DC3000 resulted in a notable reduction of the bacterial population and the complete elimination of disease symptoms (necrosis and chlorosis) in infected tomato and *Arabidopsis* plants (12, 13). The severe virulence defect in the Δ CEL mutant bacteria is caused by the deletion of the functionally redundant

¹Department of Energy Plant Research Laboratory, Department of Plant Biology, Michigan State University, East Lansing, MI 48824, USA. ²Sainsbury Laboratory, John Innes Centre, Norwich Research Park, Norwich NR4 7UH, UK.

*To whom correspondence should be addressed. E-mail: hes@msu.edu